

# Arase Observation of Simultaneous Electron Scatterings by Upper-Band and Lower-Band Chorus Emissions

著者	Kazama Y., Miyoshi Y., Kojima H., Kasahara Y., Kasahara S., Usui H., Wang B.J., Wang S.Y., Tam S.W.Y., Chang T.F., Asamura K., Matsuda S., Kumamoto A., Tsuchiya F., Kasaba Y., Shoji M., Matsuoka A., Teramoto M., Takashima T., Shinohara I.
journal or publication title	Geophysical Research Letters
volume	48
number	11
page range	e2021GL093708-1-e2021GL093708-10
year	2021-07-15
URL	<a href="http://hdl.handle.net/10228/00009047">http://hdl.handle.net/10228/00009047</a>

doi: <https://doi.org/10.1029/2021GL093708>

# Geophysical Research Letters

## RESEARCH LETTER

10.1029/2021GL093708

### Key Points:

- Arase observed intense banded chorus emissions near the magnetic equator simultaneously with an electron flux enhancement
- Parallel electron fluxes show good correlations with intensities of both the upper-band and the lower-band chorus waves
- The positive correlation indicates pitch-angle scattering of electrons by the chorus waves toward the magnetic field direction

### Correspondence to:

Y. Kazama,  
kazama.yoichi@asiaa.sinica.edu.tw







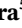

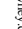
### Citation:

Kazama, Y., Miyoshi, Y., Kojima, H., Kasahara, Y., Kasahara, S., Usui, H., et al. (2021). Arase observation of simultaneous electron scatterings by upper-band and lower-band chorus emissions. *Geophysical Research Letters*, 48, e2021GL093708. <https://doi.org/10.1029/2021GL093708>

Received 6 APR 2021

Accepted 1 JUL 2021

## Arase Observation of Simultaneous Electron Scatterings by Upper-Band and Lower-Band Chorus Emissions

Y. Kazama<sup>1</sup> , Y. Miyoshi<sup>2</sup> , H. Kojima<sup>3</sup> , Y. Kasahara<sup>4</sup> , S. Kasahara<sup>5</sup> , H. Usui<sup>6</sup> , B.-J. Wang<sup>1,7</sup>, S.-Y. Wang<sup>1</sup> , S. W. Y. Tam<sup>8</sup>, T. F. Chang<sup>8</sup>, K. Asamura<sup>9</sup> , S. Matsuda<sup>9</sup> , A. Kumamoto<sup>10</sup> , F. Tsuchiya<sup>10</sup> , Y. Kasaba<sup>10</sup> , M. Shoji<sup>2</sup> , A. Matsuoka<sup>11</sup>, M. Teramoto<sup>12</sup> , T. Takashima<sup>9</sup>, and I. Shinohara<sup>9</sup> 

<sup>1</sup>Academia Sinica Institute of Astronomy and Astrophysics, Taipei, Taiwan, <sup>2</sup>Institute for Space-Earth Environmental Research, Nagoya University, Nagoya, Japan, <sup>3</sup>Research Institute for Sustainable Humanosphere, Kyoto University, Kyoto, Japan, <sup>4</sup>Graduate School of Natural Science and Technology, Kanazawa University, Kanazawa, Japan, <sup>5</sup>Department of Earth and Planetary Science, School of Science, University of Tokyo, Tokyo, Japan, <sup>6</sup>Graduate School of System Informatics, Kobe University, Kobe, Japan, <sup>7</sup>Graduate Institute of Space Science, National Central University, Taoyuan, Taiwan, <sup>8</sup>Institute of Space and Plasma Sciences, National Cheng Kung University, Tainan, Taiwan, <sup>9</sup>Institute of Space and Astronautical Science, Japan Aerospace Exploration Agency, Sagami, Japan, <sup>10</sup>Graduate School of Science, Tohoku University, Sendai, Japan, <sup>11</sup>Graduate School of Science, Kyoto University, Kyoto, Japan, <sup>12</sup>Graduate School of Engineering, Kyushu Institute of Technology, Fukuoka, Japan

**Abstract** This study reports a relation between electron flux modulations and chorus emissions by using correlation analysis. On April 18, 2017, Arase observed an enhancement of electron fluxes and intensification of banded chorus emissions at the same time. A result of the analysis shows that both the upper-band and lower-band chorus emissions have good correlations with field-aligned electron fluxes that satisfy their resonance conditions. This indicates simultaneous interactions with both the emission bands and electrons, resulting in electron pitch-angle scattering toward the magnetic field direction. In addition, low-energy electron fluxes in the perpendicular direction also show positive correlations with the chorus intensities, probably because the chorus emissions are modulated by a fluctuation of perpendicular low-energy electron fluxes.

**Plain Language Summary** Scientists have believed that pulsating auroras in the polar regions originate in precipitating electrons that are caused by a wave-particle interaction in the magnetosphere. Recent observational studies show direct evidence that chorus waves near the magnetic equator scatter local magnetospheric electrons, which are then streaming along the field line down to the ionosphere to generate aurora pulsation in response to modulation of the chorus emissions. Chorus waves usually have two distinct frequency bands, that is, upper band and lower band, but it had not been investigated that how two emission bands interact with electrons. In this study, we analyzed Arase satellite's observation data and identified good correlations between field-aligned electron fluxes and intensities of the upper-band and lower-band emissions. This result indicates that pitch-angle scattering of electrons takes place by both chorus emission bands simultaneously.

## 1. Introduction

It has been believed that pulsating auroras originate in precipitating electrons that are pitch-angle scattered by chorus waves in the magnetosphere (e.g., Ni et al., 2016; Nishimura et al., 2020). Nishimura et al. (2010) studied a relation between chorus waves and pulsating auroras by using Time History of Events and Macroscale Interactions during Substorms data. They identified the foot point of the field line of the satellite by searching the pixel of ground-based aurora images that maximizes a correlation coefficient with chorus intensities, and showed that the chorus waves in the magnetosphere and the pulsating aurora in the ionosphere were highly correlated with coefficients of  $\sim 0.88$  or  $\sim 0.71$  during time periods of several minutes. Such good correlations between pulsating auroras and chorus intensities sometimes last for an hour or even longer (Kawamura et al., 2019; Nishimura et al., 2018). Hosokawa et al. (2020) extended the chorus-aurora correlation analysis down to a sub-second time scale by using Arase (exploration of energization and radiation in geospace) (Miyoshi, Shinohara, Takashima, et al., 2018), and revealed that chorus elements and

internal modulations of the pulsating aurora were highly correlated with each other. This result has been predicted by Miyoshi et al. (2015).

It was expected that electrons are scattered into the loss cones by pitch-angle scattering due to chorus waves to generate a pulsating aurora in the ionosphere. Recently, S. Kasahara et al. (2018) presented an excellent correlation between chorus emissions and electron fluxes inside the loss cone using Arase's data. The result is the first *in-situ* measurement that indicates direct evidence of pitch-angle scattering by chorus waves. As another type of chorus-electron interactions, Landau resonance can occur with a parallel electric field component of oblique chorus waves. Agapitov et al. (2015) identified a plateau of the electron distribution at the Landau resonance energy for more than 6 h, simultaneously with chorus emissions.

Although the direct cross correlation analyses of chorus waves have already been reported with pulsating auroras (Nishimura et al., 2010) and with loss cone electrons (S. Kasahara et al., 2018), their analyses were only made for lower-band chorus (LBC) emissions. However, upper-band chorus (UBC) can also interact with electrons (Gan et al., 2020; Miyoshi et al., 2015). Simulation studies on hour-long evolution of electron distributions indicate that interactions by both UBC and LBC are needed to reproduce observed electron distributions (Ma et al., 2016; Tao et al., 2011).

Modulation of chorus emission intensity by density variation is also an interesting topic on the chorus-electron relation. Li, Bortnik, et al. (2011) showed chorus modulation events, in which a chorus intensity was enhanced by a total density increase. Similar events were reported by Nishimura et al. (2013) and Ni et al. (2014). Effects of cold electron density to growth of whistler waves were theoretically investigated (Wu et al., 2013).

In this paper, we analyze correlations between banded chorus emissions and electron fluxes for a ~2-h-long time period, in terms of wider spatial and temporal scales of chorus-electron interactions. The correlation analysis is also applied to an electron energy domain for understanding contributions of UBC and LBC emissions to the interactions with electrons.

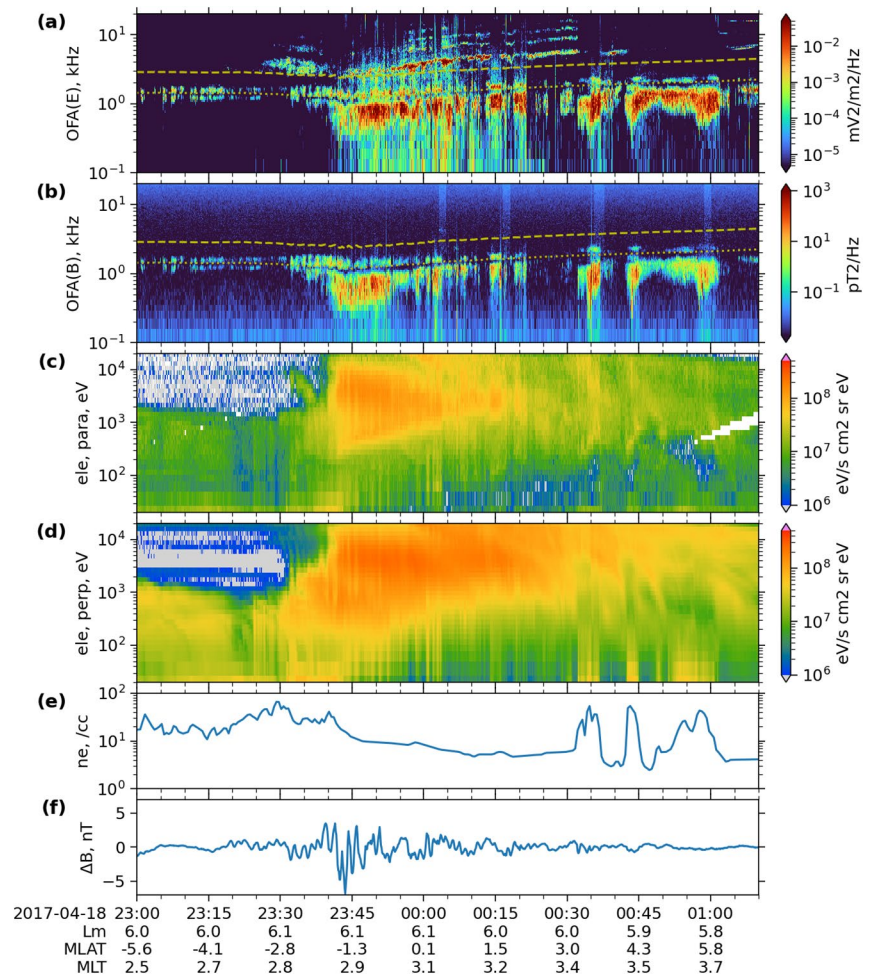
## 2. Data Sets

Low-energy (<~20 keV) electrons are measured by the LEPe instrument onboard Arase (Kazama et al., 2017). In this analysis, we use pitch angle (PA) distribution data sets with 11.25° and 5° resolutions. The 5° PA distributions are obtained by the fine channels of the instrument. The time resolutions of the data are both 8 s (spin period). Chorus waves are measured by the Onboard Frequency Analyzer (OFA) (Matsuda et al., 2018). An OFA frequency spectrum is obtained every second. For total plasma density, we carefully read upper-hybrid resonance (UHR) frequencies every 30 s measured by the High Frequency Analyzer (HFA) (Kumamoto et al., 2018). The density values were then verified by comparing with spacecraft potential and hot electron influx to the spacecraft. Both OFA and HFA belong to the Plasma Wave Experiment (PWE) instrument suite (Kasahara, Kasaba, et al., 2018). The Magnetic Field Experiment (MGF) measures magnetic fields (Matsuoka, Teramoto, Nomura, et al., 2018). A magnetic field data with 8-s time resolution were used for calculating a magnetic field fluctuation and electron cyclotron frequency.

## 3. Observation and Analysis

In this report, we analyze a chorus wave event observed at postmidnight on April 18–19, 2017. Observations of the event are summarized in Figure 1. The satellite was located at  $L_m \sim 6$  in the southern hemisphere (MLAT ~ -5.6°) at 23:00 UT, moved to the northern hemisphere and reached at MLAT ~ +5.8° at 01:00 UT. Here,  $L_m$  is the McIlwain's L-shell parameter derived from the International Geomagnetic Reference Field model. The magnetic equator crossing was at 23:59 UT.

Arase first measured an increase of electron fluxes with energies below ~600 eV, mainly in the perpendicular direction at ~23:30 UT. Around 23:40 UT, a sudden enhancement of fluxes occurred in an energy range from ~100 eV up to 20 keV both in the parallel and perpendicular directions. This flux enhancement was probably related to an electron injection during a substorm that appeared at ~23:45 UT as an energy dispersion of electrons with energies <200 keV (not shown). This indicates that a new electron population came

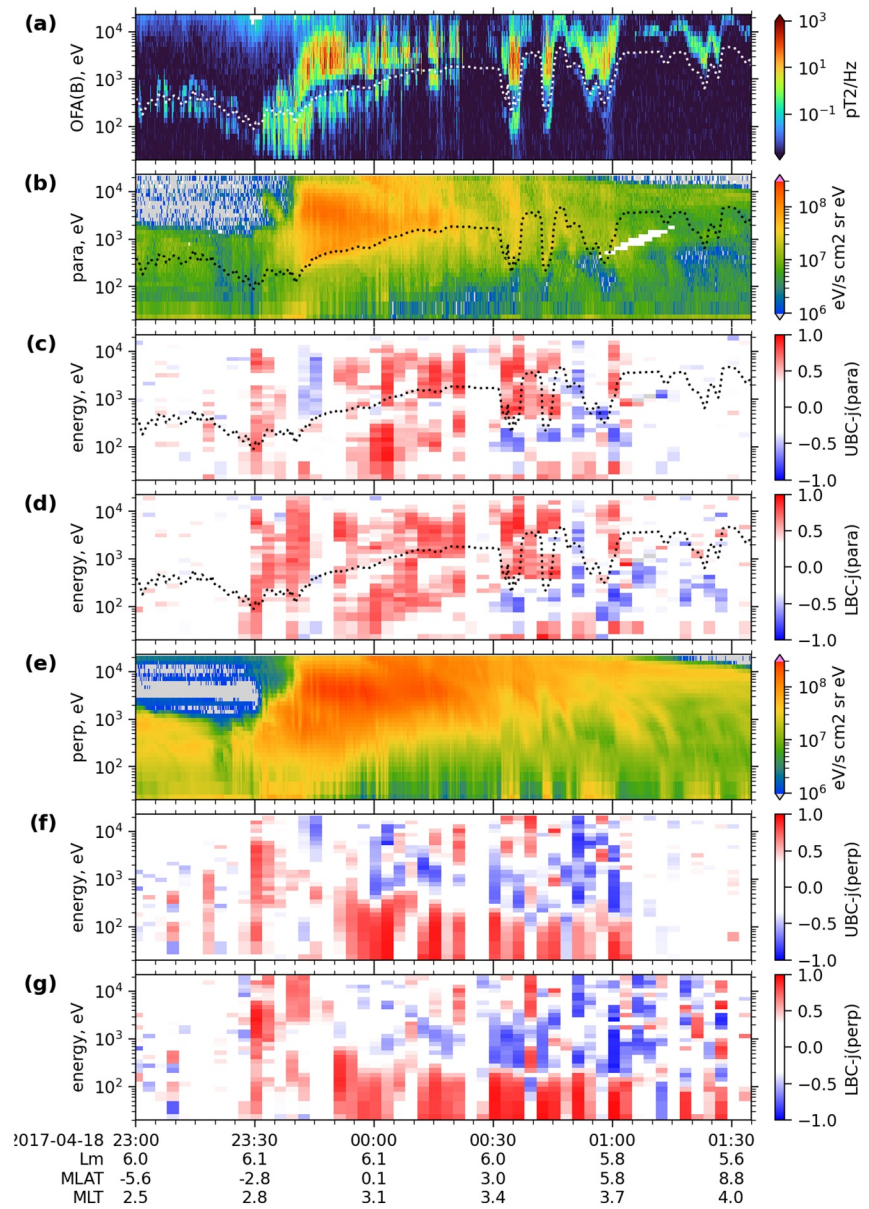


**Figure 1.** Overview of the event observed by Arase on April 18, 2017. (a and b) Electric and magnetic field wave spectrograms measured by Onboard Frequency Analyzer, with local gyrofrequency (dashed line) and half-gyrofrequency (dotted line), (c) Parallel ( $PA = 0^\circ\text{--}11.25^\circ$ ) and (d) Perpendicular ( $PA = 78.75^\circ\text{--}101.25^\circ$ ) electron energy fluxes, (e) Total plasma density based on upper-hybrid resonance frequencies measured by HFA, (f) Magnetic field fluctuation, detrended by subtracting running averages with a 10-min time window.

to the observation location. Phase space density (PSD) distributions of the electrons were of the pancake type throughout the event period. Such electron anisotropy, flux prominent in the perpendicular direction, can trigger linear growth of whistler mode waves (Kennel & Petschek, 1966). In fact, weak emissions of banded chorus waves were observed before the flux enhancement, and then intensified in response to the injection of the new electron population. The newly injected electrons are also accompanied by a magnetic field oscillation as indicated in Figure 1f. The oscillation occurred in the Pi2 frequency range. The particle injection and the Pi2 magnetic field pulsation are typical signatures of a substorm.

Here, we note that these observational signatures, that is, the electron injection, the chorus emission intensification and the magnetic field oscillation, were measured in a density fluctuation region right outside the plasmasphere. After Arase passed through the plasmopause outward around 21:50 UT, the plasma showed density irregularities ranging from a few to several tens electrons/cc. The density fluctuation continued until the inbound plasmopause crossing roughly at 02:30 UT.

To investigate chorus-electron relations, we made a correlation analysis between electron energy fluxes and chorus emission intensities. The result is summarized in Figure 2. Panel a is a magnetic field power spectrum expressed in parallel resonant energy of whistler wave (Kennel & Petschek, 1966). Here we assume



**Figure 2.** (a) Magnetic field emissions displayed in parallel resonance energy of whistler mode waves, (b) Parallel ( $PA = 0^\circ\text{--}11.25^\circ$ ) electron energy flux, (c and d) Correlations of parallel electron fluxes with the UBC and LBC emissions, respectively, (e) Perpendicular ( $PA = 78.75^\circ\text{--}101.25^\circ$ ) electron energy flux, (f and g) Correlations of perpendicular electron fluxes with the UBC and LBC emissions, respectively. Resonance energies corresponding to  $0.5f_{ce}$  are plotted with dotted lines.

purely parallel propagation of the wave. During the event period, resonant energies were within the LEPE energy range ( $\sim 20\text{--}20,000$  eV) because of the relatively high plasma densities.

In Panel b, electron energy fluxes in the parallel ( $PA = 0^\circ\text{--}11.25^\circ$ ) direction are given. Correlation coefficient (CC) spectrograms of the parallel fluxes with UBC and LBC are displayed in Panels c and d, respectively. A chorus intensity was obtained by integrating spectral power over  $f/f_{ce} = 0.1\text{--}0.5$  for LBC and  $0.5\text{--}0.9$  for UBC. Correlations were taken every 3 min with a 5-min time window. Resonance energies for  $0.5f_{ce}$  are indicated by dotted lines in the panels. Note that the CC spectrograms for the anti-parallel ( $PA = 168.75^\circ\text{--}180^\circ$ ) electrons (not shown) are similar to those for the parallel fluxes. Here, we emphasize that because the UBC and LBC emissions have already positive correlations with each other ( $CC \sim +0.5$ ), the CC spectrograms for

the UBC and the LBC have similar patterns of coefficients in time and energy if either the UBC or the LBC is correlated with electron fluxes.

Overall, we see positive correlations with CCs  $> +0.5$  for both the UBC and the LBC from  $\sim 23:30$  UT to  $\sim 01:05$  UT, which corresponds approximately to the time period when the intense UBC and LBC emissions were observed. This suggests an interaction between chorus waves and electrons; if the chorus scatter electrons toward the magnetic field direction through the interaction, the parallel electron fluxes can increase in the resonance energies, resulting in positive CCs between the chorus intensities and the electron fluxes. The previous studies by Nishimura et al. (2010) and S. Kasahara et al. (2018) focus on LBC emissions for investigating chorus-electron interactions, but in this event, the pitch-angle scattering simultaneously occurred in the energy ranges of both the UBC and the LBC. If chorus waves are well banded, CCs are expected to be low values at resonance energies for  $0.5f_{ce}$  band gaps where no intense emissions exist. Looking at the CC spectrograms closely, we notice that the  $0.5f_{ce}$  resonance energy (dotted line) follow low CC values (white pixels) from  $\sim 23:26$  UT till  $\sim 00:23$  UT. This low CC feature at  $0.5f_{ce}$  can also be seen in the anti-parallel direction.

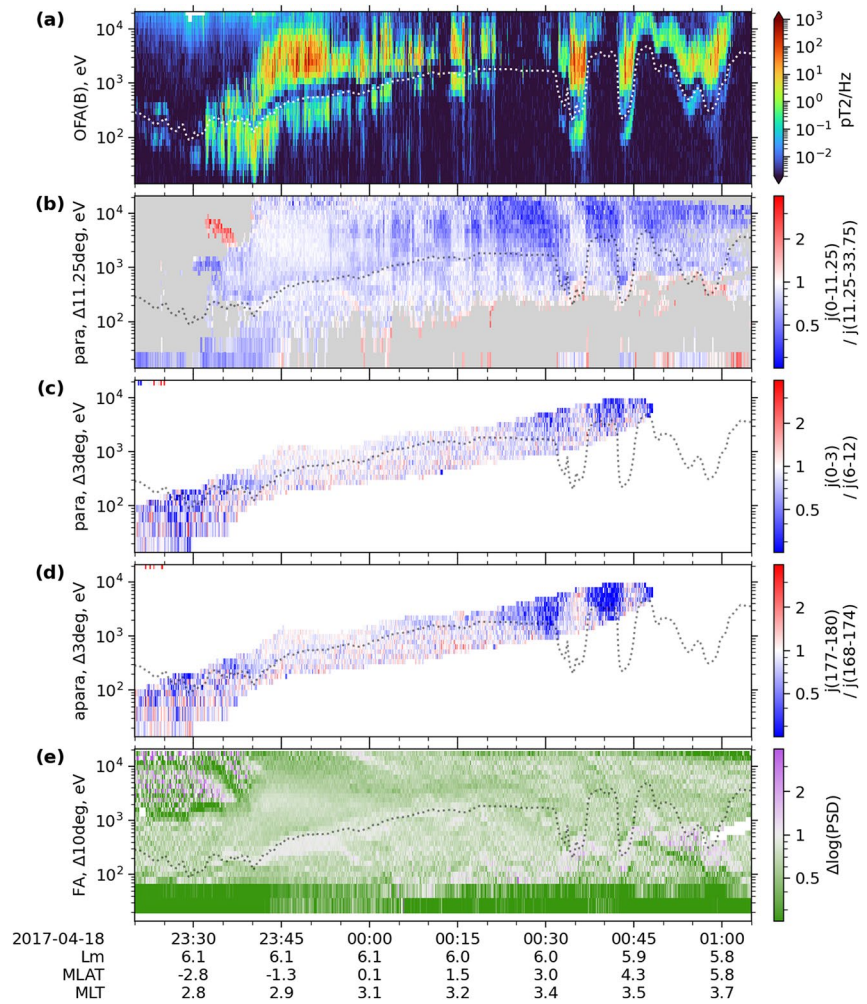
As shown in Figure 1a, electrostatic electron cyclotron harmonic (ECH) waves coexisted with the chorus waves during the event. It is known that ECH waves can also interact with electrons and scatter them in pitch angle (Fukizawa et al., 2020). According to the correlation analysis, the ECH emissions ( $f / f_{ce} = 1-4$ ) and parallel electron fluxes show a CC pattern similar to those for the UBC/LBC emissions but the CC values of the ECH are mostly negative. These negative CC values are likely to be due to anti-correlations between the ECH and the chorus waves with CCs  $\sim -0.3$  or  $-0.4$ . Therefore, contribution of the ECH waves to the electron scattering are negligible or at least less significant compared to the chorus waves in the present event.

As shown in Panels f and g, electron fluxes in the perpendicular ( $PA = 78.75^\circ-101.25^\circ$ ) direction have positive correlations with both the UBC and LBC emissions from  $\sim 23:29$  UT till  $\sim 01:05$  UT in energies below several hundred eV, differently from the parallel direction. The result indicates that perpendicular fluxes of low-energy electrons were fluctuating and the fluctuation had a close relation to the chorus waves. An anisotropic electron distribution can trigger growth of whistler mode waves (Kennel & Petschek, 1966), and thus the perpendicular electron fluctuation may modulate chorus intensities through the whistler wave generation.

If chorus waves scatter electrons toward the magnetic field direction, electron fluxes in the parallel direction are expected to increase in response to a chorus intensity enhancement. Figure 3b shows flux ratios  $j(0^\circ-11.25^\circ) / j(11.25^\circ-33.75^\circ)$  (where  $j$  is an energy flux of electrons), that is, parallel flux values relative to the neighboring PA fluxes. Data points of low flux values ( $< 10^7$  eV/s  $cm^2$  sr eV) are grayed out. A loss cone angle in this event is estimated to be about  $2^\circ-3^\circ$  by assuming a dipole magnetic field, which is much smaller than the PA width of  $11.25^\circ$ . It is clear that there is a good coincidence between the chorus waves and the flux ratios; no/weak chorus emissions correspond to flux ratios  $< 1$  (blue) in time and energy, and intense emissions to ratios  $\sim 1$  (white). This suggests that electrons in the parallel direction are originally depressed in flux, but once chorus is intensified, the waves scatter electrons to the parallel direction, resulting in an increase of the parallel electron fluxes. Here, we emphasize that the electron scatterings happened in both UBC and LBC energies.

Next, we investigate electron fluxes in/near loss cones by using the fine channel data. Panels c and d in Figure 3 are flux ratios  $j(0^\circ-3^\circ) / j(6^\circ-12^\circ)$  and  $j(177^\circ-180^\circ) / j(168^\circ-174^\circ)$ , respectively. Since the fields of view of the fine channels are limited to  $45^\circ$ , flux data are only available in a certain energy range. Points of “no flux data” are shown in white.

Before  $\sim 23:32$  UT when the chorus emissions had not been intensified, the flux ratios were mainly  $< 1$  (blue) in Panels c and d. This indicates that loss cones were not filled in the both parallel and anti-parallel directions. As the chorus emissions intensified, the ratios became  $\sim 1$  (white) because the loss cones were filled with electrons, especially after  $23:40$  UT. The loss cone filling was observed both in the parallel and anti-parallel directions until  $\sim 00:22$  UT when the intense chorus emissions disappeared. In response to weakening the chorus, the ratios came back to values  $< 1$ , except for the periods of the sudden emission

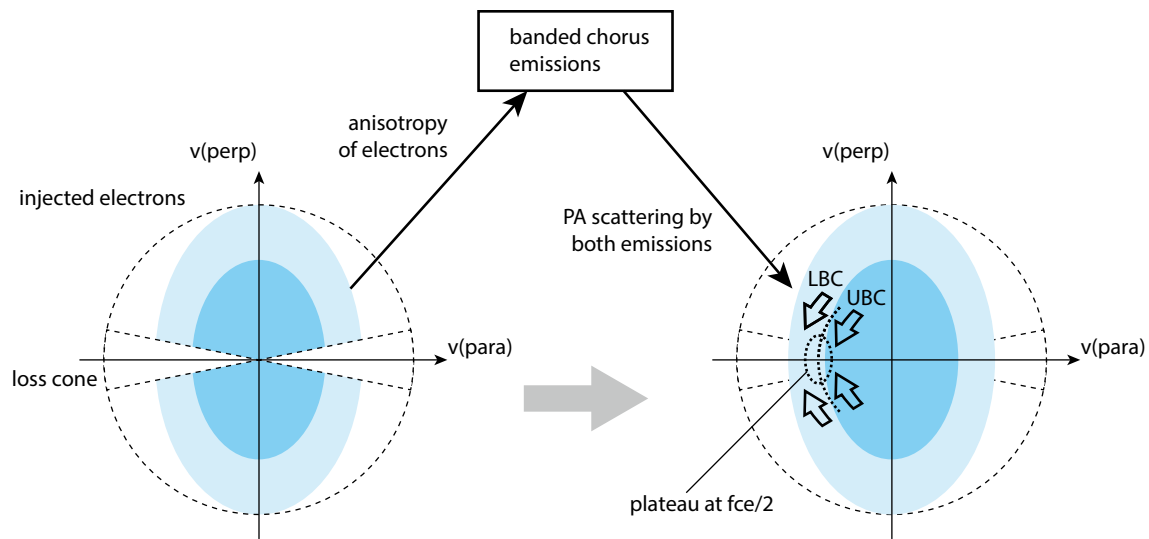


**Figure 3.** (a) Magnetic field spectrogram in parallel resonance energy of whistler mode waves, (b) Ratios of parallel fluxes  $j(0^{\circ}\text{--}11.25^{\circ}) / j(11.25^{\circ}\text{--}33.75^{\circ})$ , (c) Ratios of parallel fluxes  $j(0^{\circ}\text{--}3^{\circ}) / j(6^{\circ}\text{--}12^{\circ})$ , (d) Ratios of anti-parallel fluxes  $j(177^{\circ}\text{--}180^{\circ}) / j(168^{\circ}\text{--}174^{\circ})$ , and (e) Inclinations of an electron distribution in the field-aligned (PA < 11.25° or > 168.75°) directions,  $\text{PSD}(E_{i+1})/\text{PSD}(E_i)$ .

enhancements around 00:36 UT–00:44 UT. Note that the pitch-angle scattering occurred in energies of both the UBC and the LBC.

The flux ratios show a difference between the parallel and anti-parallel directions after ~00:22 UT; the ratios in the anti-parallel (away from the Earth, Figure 3d) direction is smaller than those in the parallel (away from the equator, Figure 3c) direction when no intense emissions were observed. Since the satellite was located in the northern hemisphere at that time, this may be caused by loss of electrons in the ionosphere, which results in lower electron fluxes inside the loss cone in the anti-parallel direction. Compared with Figure 3b, the loss cone flux ratios (Figures 3c and 3d) do not show clear modulations with the chorus waves from ~23:53 UT to ~00:22 UT. This may be because a diffusion time scale of pitch angle scattering to the loss cones for the relatively weak and intermittent chorus emissions is longer than the durations of the waves. Therefore, the loss cone fluxes are not always determined by an instantaneous interaction with waves at the observation point, and a time history of interactions should be considered.

The chorus waves observed were well banded as distinct UBC and LBC, and thus no emissions existed at  $0.5f_{ce}$ . If there are no emissions at a half-gyrofrequency, it is expected that electrons at energies corresponding to  $0.5f_{ce}$  do not experience any pitch-angle scattering, which can result in a modulation of PSD at the half-gyrofrequency. To investigate such modulations, a ratio of PSDs,  $\text{PSD}(E_{i+1})/\text{PSD}(E_i)$  is plotted



**Figure 4.** Summary of the observations of the chorus event in this report.

in Figure 3e, where  $E$  is an electron energy. Mostly, the ratios show negative (green) as the distribution decreases monotonically in energy. However, we see ratios close to  $\sim 1$  (white) at  $0.5f_{ce}$  from  $\sim 23:35$  UT to  $\sim 00:13$  UT (magnetic equator crossing at  $\sim 23:59$  UT). This indicates that the distribution is of a plateau-like shape at an energy corresponding to  $0.5f_{ce}$  near the magnetic equator. We will discuss this point in the next section.

#### 4. Summary and Discussion

In this study, we investigated a relation between electron fluxes and chorus emissions by using Arase's observation data. The results of the data analysis can be summarized as follows:

1. Arase observed chorus wave intensifications when a new electron population were injected to the satellite location
2. The intensities of the UBC and LBC emissions were positively correlated with (a) the parallel electron fluxes and (b) the perpendicular low-energy electron fluxes
3. Parallel electron fluxes increased and loss cones were filled with electrons when the chorus waves were intensified.

Here is our interpretation that can explain the results. See also Figure 4.

1. A dense and anisotropic electron population is injected and trigger generation of whistler mode waves, which finally become banded chorus emissions
2. A fluctuation of perpendicular electron fluxes in low energies changes the anisotropy and/or the density of electrons, resulting in modulating the chorus emission intensities
3. The chorus waves scatter electrons toward the magnetic field direction, and consequently electron fluxes in the parallel direction increase and the loss cone is filled with electrons.

We emphasize that both the UBC and the LBC simultaneously interact with electrons at their resonance energies for more than an hour, according to the correlation analysis.

In this report, we calculated resonance energies under assumption that the chorus wave propagated purely along the field line. A wave normal angle analysis indicates that the LBC emissions observed from 23:30 UT to 00:10 UT have  $\sim 0^\circ$ – $15^\circ$  of propagation angles, and thus the parallel propagation assumption is reasonable. For the other emissions, we could not estimate wave normal angles accurately because of small planarity of the waves. In fact, even although the wave normal angle is  $30^\circ$ , a significant difference of resonance energy appears only in  $f/f_{ce} > \sim 0.8$  (see Figure 1 in Artemyev et al., 2016), corresponding to



electron energies below  $\sim 10$  eV in the case of this event. Therefore, we think that the assumption of parallel propagation is applicable here.

As seen in Figure 3e, electron PSD distributions sometimes show a plateau-like feature at  $0.5f_{ce}$  in the parallel direction, simultaneously with intensified banded chorus emissions near the equator. Recently Li et al. (2019) reported plateau features in electron distributions observed by the Van-Allen Probes, and conclude that such feature results from Landau resonance of electrons with whistler waves excited initially at the equator. Once a plateau has been formed in the distribution, the electron anisotropy at the plateau's energy is reduced and further wave growth is suppressed at  $0.5f_{ce}$ , which finally causes banded chorus emissions. Thus, the plateau feature observed by Arase can be attributed to the generation process of banded chorus, according to their report. Once a whistler wave has grown to be a banded chorus wave, both the UBC and LBC emissions scatter electrons toward the magnetic field direction, and then parallel electron fluxes increase, as shown in this study. As a consequence, parallel PSDs under/above the  $0.5f_{ce}$  energy are enhanced, which may suppress the plateau in the distribution. This implies that an effect of the electron scattering by chorus waves may contribute to developing the chorus waves themselves.

Another possibility of generating a plateau distribution is proposed by Artemyev and Mourenas (2020), in which a plateau is formed by electron acceleration due to kinetic alfvén waves or time domain structures, or by ionospheric outflow. This may agree with the plateaus existing continuously even during the time periods when no chorus was observed (e.g., 00:12–00:14 UT, 00:40–00:42 UT). According to Artemyev and Mourenas (2020), generation of slightly oblique LBC waves is favored if their Landau resonance energies are at the plateau because the Landau damping is suppressed (Note that in this event, the minimum Landau resonance energy is almost same as the energy of the cyclotron resonance with  $0.5f_{ce}$ , dotted line in Figure 3e). Based on this interpretation, the intense LBC emissions from  $\sim 23:40$  UT to  $\sim 23:55$  UT and more clearly at  $\sim 00:36$  UT,  $\sim 00:44$  UT and  $\sim 00:58$  UT can be explained as a coincidence between the Landau resonance energy and the plateau energy due to the density variations.

In the correlation analysis, positive correlations were found between the chorus intensities and the low-energy ( $< \sim 300$  eV) perpendicular electron fluxes. This means that the low-energy perpendicular fluxes were fluctuating in time. We consider that the chorus emissions were modulated by the flux fluctuation through a parameter that controls the whistler wave generation process. It is not obvious what drove the flux fluctuation of low-energy electrons in the perpendicular direction. Li, Thorne, et al. (2011) and Xia et al. (2016) reported intensity modulations of whistler mode waves driven by Pc4-5 pulsations. In the present event, a Pi2 pulsation was clearly observed along with the electron injection. To the authors' knowledge, there are no studies of whistler wave modulation by a Pi2 pulsation, but the same mechanism can work for Pi2 pulsation as reported for continuous ULF pulsations. However, we note that the Pi2 pulsation observed is not well correlated with the chorus intensities (not shown).

Besides ULF pulsations, Li, Bortnik, et al. (2011) pointed out that a density fluctuation can also modulate chorus waves. Before  $\sim 00:25$  UT, CCs between the chorus emissions and the total plasma density were roughly within  $\pm 0.5$  and are not systematic. After  $\sim 00:25$  UT, the CCs increased up to  $\sim +0.77$  (UBC) and  $\sim +0.89$  (LBC). Notably, the chorus intensifications and the density enhancements simultaneously appeared around  $\sim 00:35$  UT,  $\sim 00:43$  UT and  $\sim 00:58$  UT. This simultaneous appearance is similar to the density enhancement events shown by Li, Bortnik, et al. (2011), in which a higher plasma density lowers the resonance energy for more electrons to contribute to wave growth. In addition to the density enhancements, electron anisotropy were also enhanced in low energies ( $< \sim 500$  eV) during the periods of the density enhancements (not shown). Both the density and anisotropy enhancements can contribute to the chorus intensification. Furthermore, growth of the chorus waves could also be modulated by decrease/increase of their Landau damping related to plateau presence/absence in the corresponding energy range as a plasma density increase/decrease (Artemyev & Mourenas, 2020), as previously observed for highly oblique chorus waves (Li et al., 2016; Mourenas et al., 2015).

In this study, we showed the observation data that suggested that electrons were scattered in pitch angle toward the magnetic field direction by both the UBC and LBC simultaneously. As a result of the pitch-angle scattering, electron fluxes in the loss cone increase in energies corresponding to both the UBC and LBC emissions. Such loss-cone electrons are then expected to precipitate into the ionosphere to cause a pulsating

auroras (Hosokawa et al., 2020; S. Kasahara et al., 2018; Nishimura et al., 2010). Miyoshi et al. (2015) reported two distinct populations of precipitating electrons observed by the low-altitude orbiting satellite Reimei, simultaneously with pulsating auroras below the observation point. Based on the observations and the computer simulation, they conclude that downward electrons observed in the higher and lower energies originate from LBC and UBC activities in the magnetosphere, respectively, and the energy gap between the two populations corresponds to a gap of the banded chorus emissions. Their conclusion agrees with our result that banded chorus emissions enhance field-aligned electrons in the two energy ranges. Simultaneous observations of electrons at multiple locations such as the magnetic equator and a low altitude will be future work.

### Data Availability Statement

The data used in this study are as follows: LEPe data are level-1a v6 (calibrated, identical to level-2 v02\_02 (Wang et al., 2018)), OFA spectral data are level-2 v02\_01 (Kasahara, Kojima, et al., 2018), HFA spectral data are level-2 v01\_01 (Kasahara, Kumamoto, et al., 2018), MGF magnetic field data are level-2 v03.04 (Matsuo-ka, Teramoto, Imajo, et al., 2018), and orbit data are level-2 v03 (Miyoshi, Shinohara, & Jun 2018). All the data were calibrated/evaluated by the instrument teams. Arase (ERG) data are archived by the ERG Science Center operated by ISAS/JAXA and ISEE/Nagoya University (Miyoshi, Hori, et al., 2018). The data used in this study are available at [https://ergsc.isee.nagoya-u.ac.jp/data\\_info/erg.shtml.en](https://ergsc.isee.nagoya-u.ac.jp/data_info/erg.shtml.en). The data were retrieved by SPEDAS (Space Physics Environment Data Analysis Software) (Angelopoulos et al., 2019).

### Acknowledgments

This work was supported by Ministry of Science and Technology of Taiwan under Contract No. MOST 106-2111-001-011, and by Japan Society for the Promotion of Science, KAKENHI Grant Numbers 15H05815, 15H05747, 16H06286, 17H00728, 20H01959, 17H06140 and 21H04520.

### References

- Agapitov, O. V., Artemyev, A. V., Mourenas, D., Mozer, F. S., & Krasnoselskikh, V. (2015). Nonlinear local parallel acceleration of electrons through Landau trapping by oblique whistler mode waves in the outer radiation belt. *Geophysical Research Letters*, *42*(23), 10140–10149. <https://doi.org/10.1002/2015GL066887>
- Angelopoulos, V., Cruce, P., Drozdov, A., Grimes, E. W., Hatzigeorgiu, N., King, D. A., et al. (2019). The space physics environment data analysis system (SPEDAS). *Space Science Reviews*, *215*(1), 9. <https://doi.org/10.1007/s11214-018-0576-4>
- Artemyev, A., Agapitov, O., Mourenas, D., Krasnoselskikh, V., Shastun, V., & Mozer, F. (2016). Oblique whistler-mode waves in the earth's inner magnetosphere: Energy distribution, origins, and role in radiation belt dynamics. *Space Science Reviews*, *200*(1), 261–355. <https://doi.org/10.1007/s11214-016-0252-5>
- Artemyev, A. V., & Mourenas, D. (2020). On whistler mode wave relation to electron field-aligned plateau populations. *Journal of Geophysical Research: Space Physics*, *125*(3), e2019JA027735. <https://doi.org/10.1029/2019JA027735>
- Fukizawa, M., Sakanoi, T., Miyoshi, Y., Kazama, Y., Katoh, Y., Kasahara, Y., et al. (2020). Pitch-angle scattering of inner magnetospheric electrons caused by ECH waves obtained with the Arase satellite. *Geophysical Research Letters*, *47*(23), e2020GL089926. <https://doi.org/10.1029/2020GL089926>
- Gan, L., Li, W., Ma, Q., Artemyev, A. V., & Albert, J. M. (2020). Unraveling the formation mechanism for the bursts of electron butterfly distributions: Test particle and quasilinear simulations. *Geophysical Research Letters*, *47*(21), e2020GL090749. <https://doi.org/10.1029/2020GL090749>
- Hosokawa, K., Miyoshi, Y., Ozaki, M., Oyama, S.-I., Ogawa, Y., Kurita, S., et al. (2020). Multiple time-scale beats in aurora: Precise orchestration via magnetospheric chorus waves. *Scientific Reports*, *10*(1), 3380. <https://doi.org/10.1038/s41598-020-59642-8>
- Kasahara, S., Miyoshi, Y., Yokota, S., Mitani, T., Kasahara, Y., Matsuda, S., et al. (2018). Pulsating aurora from electron scattering by chorus waves. *Nature*, *554*(7692), 337–340. <https://doi.org/10.1038/nature25505>
- Kasahara, Y., Kasaba, Y., Kojima, H., Yagitani, S., Ishisaka, K., Kumamoto, A., et al. (2018). The plasma wave experiment (PWE) on board the Arase (ERG) satellite. *Earth Planets and Space*, *70*(1), 86. <https://doi.org/10.1186/s40623-018-0842-4>
- Kasahara, Y., Kojima, H., Matsuda, S., Ozaki, M., Yagitani, S., Shoji, M., & Shinohara, I. (2018). *The PWE/OFA instrument level-2 spectrum data of exploration of energization and radiation in geospace (ERG) Arase satellite*. <https://doi.org/10.34515/DATA.ERG-08000>
- Kasahara, Y., Kumamoto, A., Tsuchiya, F., Matsuda, S., Shoji, M., Nakamura, S., & Miyoshi, Y. (2018). *The PWE/HFA instrument level-2 spectrum data of exploration of energization and radiation in geospace (ERG) Arase satellite*. <https://doi.org/10.34515/DATA.ERG-10000>
- Kawamura, S., Hosokawa, K., Kurita, S., Oyama, S., Miyoshi, Y., Kasahara, Y., et al. (2019). Tracking the region of high correlation between pulsating aurora and chorus: Simultaneous observations with Arase satellite and ground-based all-sky imager in Russia. *Journal of Geophysical Research: Space Physics*, *124*(4), 2769–2778. <https://doi.org/10.1029/2019JA026496>
- Kazama, Y., Wang, B.-J., Wang, S.-Y., Ho, P. T. P., Tam, S. W. Y., Chang, T.-F., et al. (2017). Low-energy particle experiments-electron analyzer (LEPe) onboard the Arase spacecraft. *Earth Planets and Space*, *69*(1), 165. <https://doi.org/10.1186/s40623-017-0748-6>
- Kennel, C. F., & Petschek, H. E. (1966). Limit on stably trapped particle fluxes. *Journal of Geophysical Research*, *71*(1), 1–28. <https://doi.org/10.1029/JZ071i001p00001>
- Kumamoto, A., Tsuchiya, F., Kasahara, Y., Kasaba, Y., Kojima, H., Yagitani, S., et al. (2018). High frequency analyzer (HFA) of plasma wave experiment (PWE) onboard the Arase spacecraft. *Earth Planets and Space*, *70*(1), 82. <https://doi.org/10.1186/s40623-018-0854-0>
- Li, J., Bortnik, J., An, X., Li, W., Angelopoulos, V., Thorne, R. M., et al. (2019). Origin of two-band chorus in the radiation belt of Earth. *Nature Communications*, *10*(1), 4672. <https://doi.org/10.1038/s41467-019-12561-3>
- Li, W., Bortnik, J., Thorne, R. M., Nishimura, Y., Angelopoulos, V., & Chen, L. (2011). Modulation of whistler mode chorus waves: 2. Role of density variations. *Journal of Geophysical Research*, *116*(A6), A06206. <https://doi.org/10.1029/2010JA016313>
- Li, W., Mourenas, D., Artemyev, A. V., Bortnik, J., Thorne, R. M., Kletzing, C. A., et al. (2016). Unraveling the excitation mechanisms of highly oblique lower band chorus waves. *Geophysical Research Letters*, *43*(17), 8867–8875. <https://doi.org/10.1002/2016GL070386>

- Li, W., Thorne, R. M., Bortnik, J., Nishimura, Y., & Angelopoulos, V. (2011). Modulation of whistler mode chorus waves: 1. Role of compressional Pc4-5 pulsations. *Journal of Geophysical Research*, *116*(A6), A06205. <https://doi.org/10.1029/2010JA016312>
- Ma, Q., Mourenas, D., Artemyev, A., Li, W., Thorne, R. M., & Bortnik, J. (2016). Strong enhancement of 10–100 keV electron fluxes by combined effects of chorus waves and time domain structures. *Geophysical Research Letters*, *43*(10), 4683–4690. <https://doi.org/10.1002/2016GL069125>
- Matsuda, S., Kasahara, Y., Kojima, H., Kasaba, Y., Yagitani, S., Ozaki, M., et al. (2018). Onboard software of plasma wave experiment aboard Arase: Instrument management and signal processing of waveform capture/onboard frequency analyzer. *Earth Planets and Space*, *70*(1), 75. <https://doi.org/10.1186/s40623-018-0838-0>
- Matsuoka, A., Teramoto, M., Imajo, S., Kurita, S., Miyoshi, Y., & Shinohara, I. (2018). The MGF instrument level-2 spin-averaged magnetic field data of exploration of energization and radiation in geospace (ERG) Arase satellite. <https://doi.org/10.34515/DATA.ERG-06001>
- Matsuoka, A., Teramoto, M., Nomura, R., Nosé, M., Fujimoto, A., Tanaka, Y., et al. (2018). The ARASE (ERG) magnetic field investigation. *Earth Planets and Space*, *70*(1), 43. <https://doi.org/10.1186/s40623-018-0800-1>
- Miyoshi, Y., Hori, T., Shoji, M., Teramoto, M., Chang, T. F., Segawa, T., et al. (2018). The ERG science center. *Earth Planets and Space*, *70*(1), 96. <https://doi.org/10.1186/s40623-018-0867-8>
- Miyoshi, Y., Saito, S., Seki, K., Nishiyama, T., Kataoka, R., Asamura, K., et al. (2015). Relation between fine structure of energy spectra for pulsating aurora electrons and frequency spectra of whistler mode chorus waves. *Journal of Geophysical Research: Space Physics*, *120*(9), 7728–7736. <https://doi.org/10.1002/2015JA021562>
- Miyoshi, Y., Shinohara, I., & Jun, C.-W. (2018). The level-2 orbit data of exploration of energization and radiation in geospace (ERG) Arase satellite. <https://doi.org/10.34515/DATA.ERG-12000>
- Miyoshi, Y., Shinohara, I., Takashima, T., Asamura, K., Higashio, N., Mitani, T., et al. (2018). Geospace exploration project ERG. *Earth Planets and Space*, *70*(1), 101. <https://doi.org/10.1186/s40623-018-0862-0>
- Mourenas, D., Artemyev, A. V., Agapitov, O. V., Krasnoselskikh, V., & Mozer, F. S. (2015). Very oblique whistler generation by low-energy electron streams. *Journal of Geophysical Research: Space Physics*, *120*(5), 3665–3683. <https://doi.org/10.1002/2015JA021135>
- Ni, B., Bortnik, J., Nishimura, Y., Thorne, R. M., Li, W., Angelopoulos, V., et al. (2014). Chorus wave scattering responsible for the Earth's dayside diffuse auroral precipitation: A detailed case study. *Journal of Geophysical Research: Space Physics*, *119*(2), 897–908. <https://doi.org/10.1002/2013JA019507>
- Ni, B., Thorne, R. M., Zhang, X., Bortnik, J., Pu, Z., Xie, L., et al. (2016). Origins of the Earth's diffuse auroral precipitation. *Space Science Reviews*, *200*(1), 205–259. <https://doi.org/10.1007/s11214-016-0234-7>
- Nishimura, Y., Bortnik, J., Li, W., Angelopoulos, V., Donovan, E. F., & Spanswick, E. L. (2018). Comment on “pulsating auroras produced by interactions of electrons and time domain structures” by Mozer et al. *Journal of Geophysical Research: Space Physics*, *123*(3), 2064–2070. <https://doi.org/10.1002/2017JA024844>
- Nishimura, Y., Bortnik, J., Li, W., Thorne, R. M., Lyons, L. R., Angelopoulos, V., et al. (2010). Identifying the driver of pulsating aurora. *Science*, *330*(6000), 81–84. <https://doi.org/10.1126/science.1193186>
- Nishimura, Y., Bortnik, J., Li, W., Thorne, R. M., Ni, B., Lyons, L. R., et al. (2013). Structures of dayside whistler-mode waves deduced from conjugate diffuse aurora. *Journal of Geophysical Research: Space Physics*, *118*(2), 664–673. <https://doi.org/10.1029/2012JA018242>
- Nishimura, Y., Lessard, M. R., Katoh, Y., Miyoshi, Y., Grono, E., Partamies, N., et al. (2020). Diffuse and pulsating aurora. *Space Science Reviews*, *216*(1), 4. <https://doi.org/10.1007/s11214-019-0629-3>
- Tao, X., Thorne, R. M., Li, W., Ni, B., Meredith, N. P., & Horne, R. B. (2011). Evolution of electron pitch angle distributions following injection from the plasma sheet. *Journal of Geophysical Research*, *116*(A4), A04229. <https://doi.org/10.1029/2010JA016245>
- Wang, S.-Y., Kazama, Y., Jun, C.-W., Chang, T.-F., Hori, T., Miyoshi, Y., & Shinohara, I. (2018). The LEPe instrument level-2 3-d flux data of exploration of energization and radiation in geospace (ERG) Arase satellite. <https://doi.org/10.34515/DATA.ERG-04001>
- Wu, S., Denton, R. E., & Li, W. (2013). Effects of cold electron density on the whistler anisotropy instability. *Journal of Geophysical Research: Space Physics*, *118*(2), 765–773. <https://doi.org/10.1029/2012JA018402>
- Xia, Z., Chen, L., Dai, L., Claudepierre, S. G., Chan, A. A., Soto-Chavez, A. R., & Reeves, G. D. (2016). Modulation of chorus intensity by ULF waves deep in the inner magnetosphere. *Geophysical Research Letters*, *43*(18), 9444–9452. <https://doi.org/10.1002/2016GL070280>